Microchimica Acta (2020) 187:444
https://doi.org/10.1007/s00604-020-04400-w

ORIGINAL PAPER

Determination of miRNAs in serum of cancer patients with a label- and enzyme-free voltammetric biosensor in a single 30-min step

Mohamed Zouari[1,2] · Susana Campuzano[3] · José M. Pingarrón[3] · Noureddine Raouafi[1]

Received: 3 April 2020 / Accepted: 17 June 2020

Abstract

The preparation of an integrated biosensor for the easy, fast, and sensitive determination of miRNAs is described based on a direct hybridization format and a label-free voltammetric detection. The biosensor involves a disposable carbon electrode substrate doubly nanostructured with reduced graphene oxide (rGO) and AuNPs modified with pyrene carboxylic acid (PCA) and 6-ferrocenylhexanethiol (Fc-SH), respectively. A synthetic amino terminated DNA capture probe was covalently immobilized on the CO_2H moieties of PCA/rGO, while Fc-SH was used as a signaling molecule. Differential pulse voltammetry was employed to record the decrease in the oxidation peak current of Fc after the hybridization due to the hindering of the electron transfer upon the formation of the DNA-RNA duplex on the electrode surface. The stepwise biosensor preparation was characterized by surface and electrochemical techniques showing the role played by each biosensor component as well as the reliability of the target miRNA determination. The determination of the oncogene miRNA-21 synthetic target allowed quantification in the low femtomolar range (LOD of 5 fM) with a high discrimination of single-base mismatched sequences in a single 30-min incubation step. The bioplatform allowed the determination of the target miRNA in a small amount of total RNA extracted from breast cancer (BC) cells or directly in serum samples collected from BC patients without the need for prior extraction, purification, amplification, or reverse transcription of the genetic material and with no matrix effect.

Keywords miRNA-21 · Electrochemical biosensor · Label-free · Serum samples · Nanomaterial · Breast cancer

Introduction

Dysregulation of microRNAs (miRNAs), naturally occurring small (about 22 nucleotides long) RNA transcripts that are not transcribed into proteins but regulate the transcription, stability, or translation of protein-coding genes in the mammalian genome [1], is associated with cancer initiation, development, and metastasis as well as with tumor response to treatments. The apparent stability of miRNAs in archived patient material (formalin-fixed paraffin-embedded biopsies) and easily accessible body fluids (serum, sputum, and pulmonary lavage) triggers research interest in their use as particularly interesting minimally invasive biomarkers for early cancer detection and personalized therapies monitoring [2–6]. However, the simple, precise, and low-cost quantification of miRNAs is still challenging because of their tiny size, and the high sensitivity (fM-pM range in clinical samples) [7] and specificity required against a background of overwhelmingly abundant molecules including non-target RNAs with sequence and size similarity. Furthermore, the difference of miRNAs expression between healthy individuals and patients is small [8].

Currently, the main strategies for miRNAs identification and quantification include real-time fluorescent quantitative polymerase chain reaction (RT-qPCR), northern blotting, microarrays, and deep sequencing of transcriptome (RNAseq). These techniques are accurate but suffer from poor sensitivity and low anti-interference, which avoids direct detection in biofluids [8]. Moreover, these techniques, although routinely performed by technicians in laboratory settings, require

Electronic supplementary material The online version of this article (https://doi.org/10.1007/s00604-020-04400-w) contains supplementary material, which is available to authorized users.

✉ Noureddine Raouafi
noureddine.raouafi@fst.utm.tn

[1] Sensors and Biosensors Group, Analytical Chemistry and Electrochemistry Lab (LR99ES15), Chemistry Department, University of Tunis El Manar, 2092 Tunis El Manar, Tunisia

[2] Institut Pasteur de Tunis, 13 place Pasteur, 1002 Tunis, Tunisia

[3] Departamento de Química Analítica, Facultad de CC. Químicas, Universidad Complutense de Madrid, E–28040 Madrid, Spain

expensive instrumentation which made them not suitable for either low resource or decentralized settings [7, 9, 10].

In recent years, electrochemical biosensors have attracted great interest for the determination of miRNAs due to the inherent advantages of low cost, simplicity of use, response rapidity, easy miniaturization, and multiplexing and mass fabrication capability [7, 10]. To achieve the required selectivity, these biosensors involve hybridization events of the target miRNA with complementary synthetic probes employing either label-based or label-free methods. The excellent performance imparted by the current electrochemical biosensing is the result of successful and ingenious combinations of bioassay formats and the use of different functional single or hybrid nanomaterials providing enhanced surface area and catalytic properties [9]. However, in most cases, the construction of these biosensors involves multiple steps and/or lasting protocols for the preparation and functionalization of the nanomaterials or the electrode surface [7]. Therefore, in recent years, label-free electrochemical strategies measuring the difference between the voltammetric responses associated with different redox probes such as thionine, methylene blue, ferrocene, or porous silver nanofoam both in solution or attached to the electrode surface, before and after hybridization with the target miRNA, have attracted wide attention [10]. In the last few years, electrochemical biosensors involving label-free determination of miRNAs at clinically relevant sensitivity have been reported [11–15]. However, they still require multiple steps to carry out the determination [13], laborious protocols for the preparation of the biosensing surface [11, 14], and/or the bioconjugates used for amplification purposes [15]. Furthermore, their applicability for the determination of endogenous miRNAs contents in poorly diluted samples has not been widely demonstrated.

To face these demands, in this work, we report a simple and rapid direct hybridization assay for the label-free determination of miRNAs using electrodes double nanostructured with rGO and AuNPs modified with pyrene carboxylic acid (PCA) and 6-ferrocenylhexanethiol (Fc-SH), respectively. The PCA/rGO was used as scaffold for the covalent immobilization of an NH_2 terminated synthetic DNA capture probe (NH_2-DNACp) complementary to the target miRNA (miR-21, an oncomiRNA in most cancers). In addition, due to the electron transfer between Fc and the electrode surface, the Fc oxidation peak current was sensitively monitored using differential pulse voltammetry (DPV). After a 30-min hybridization with miRNA-21, the duplex DNA-RNA formed at the NH_2-DNACp/PCA/Fc-SH/AuNPs/rGO/SPCE greatly hindered the electron transfer on the electrode surface and caused a decrease in the DPV Fc oxidation peak. The prepared bioplatform exhibited a high sensitivity (in the low fM level) and selectivity (even to a single mismatch sequence) for the determination of the target miRNA in a direct reading of serum samples.

Materials and methods

Apparatus and electrodes

Cyclic voltammetry (CV), DPV, chronoamperometry, and electrochemical impedance spectroscopy (EIS) were performed with a Metrohm Autolab PGSTAT M204 electrochemical workstation using the Nova® v1.11 software. The transducers employed were screen-printed carbon electrodes (SPCEs, DRP-110 consisting of a 4-mm diameter carbon working electrode, WE, a carbon counter electrode, and an Ag pseudo-reference electrode). The SPCEs and the specific cable connector (DRP-CAC) were purchased from Dropsens S.L. (Oviedo, Spain).

A Bunsen AGT-9 Vortex for homogenization of the solutions, an ultrasonic bath Fisherbrand™, a Raypa steam sterilizer, a block heater (Stuart), a biological safety cabinet Telstar Biostar, and a NanoDrop® ND-1000 spectrophotometer (NanoDrop Technologies used to evaluate the quality and quantity of the extracted cellular RNA) were also employed.

Scanning electron microscopy (SEM) was performed using a field emission scanning electron microscope JEOL JSM-6360, and the energy-dispersive X-ray (EDX) characterization was made using a transmission electron microscope (FEI TECNAI G^2 F20 HRTEM) operating at 120 and 200 kV.

Reagents and solutions

All reagents used were of the highest available grade. NaH_2PO_4, Na_2HPO_4, NaCl, Na_2CO_3, $NaHCO_3$, KCl, and methanol were purchased from Scharlab. Tris-(hydroxymethyl)aminomethane hydrochloride (Tris-HCl), mercaptohexanol (MCH), H_2SO_4, tetrachloroauric acid trihydrate ($HAuCl_4 \cdot 3H_2O$), ethylenediaminetetraacetic acid (EDTA), ethanol, potassium ferrocyanide ($K_4Fe(CN)_6$), potassium ferricyanide ($K_3Fe(CN)_6$), bovine serum albumin (BSA), 6-ferrocenylhexanethiol (Fc-SH), 1-pyrenoacetic acid (PCA),N-(3-dimethylaminopropyl)-N′-ethylcarbodimide (EDC), and N-hydroxysuccinimide (NHS) were purchased from Merck, and graphene oxide (GO) was purchased from Orion High Technologies. All used oligonucleotides (Table 1) were purchased from Merck and, after reconstitution at a final concentration of 100 μM, were stored in small aliquots at − 80 °C.

The following buffer solutions were prepared with Milli-Q water (18 MΩ cm at 25 °C) and sterilized after their preparation to avoid RNase degradation: 0.1 M NaH_2PO_4/Na_2HPO_4 of pH 7.0; 0.1 M $NaHCO_3/Na_2CO_3$ buffer of pH 9.0; 0.01 M phosphate buffer solution containing 137 mM NaCl and 2.7 mM KCl (phosphate-buffered saline, PBS) of pH 7.5; 10 mM Tris-HCl supplemented with 1 mM EDTA; and 0.3 M NaCl (Tris-EDTA buffer) of pH 8.0 and 0.05 M phosphate buffer of pH 6.0.

Table 1 Sequences of the synthetic oligonucleotides used in this work

Oligonucleotide	Sequence (5′ → 3′)
Amino-terminated DNA probe (NH_2-DNACp)	NH_2-$(CH_2)_3$-TCAACATCAGT
Target miRNA-21	UAGCUUAUCAGACUGAUGUUGA
1-mismatched miRNA-21 (1-m)	UAGCUUAUAAGACUGAUGUUGA
miRNA-451 (NC)	UUGAGUCAUUACCAUUGCAAA

1-m and *NC*, sequences with a different single-base mismatch (underlined) and fully non-complementary to the target miRNA

Preparation of NH_2-DNACp/PCA/Fc-SH/AuNPs/rGO/SPCE recognition interface

Before modification of the SPCEs, they were activated by depositing a 50 μL drop of a 0.1 M Na_2HPO_4/NaH_2PO_4 buffer solution (pH 7.0) covering the three electrodes of the SPCE and applying a + 1.7 V potential (vs. the Ag pseudo-reference electrode) for 60 s [16]. After washing the electrodes with Milli-Q water and allowing drying in air, the SPCEs were modified with electrodeposited rGO. To do this, 50 μL of a 1 mg mL^{-1} GO dispersion (prepared in 0.1 M $Na_2CO_3/NaHCO_3$, pH 9.0, and sonicated until homogenization) was deposited covering the three electrodes, and 10 cyclic voltammograms between − 0.40 and + 0.60 V (vs the Ag pseudo-reference electrode) at 50 mV s^{-1} [17] were carried out. Thereafter, the electrodes were washed with Milli-Q H_2O and allowed drying on air.

Then, AuNPs were electrodeposited on the rGO/SPCEs by applying a − 0.5 V potential (vs. the Ag pseudo-reference electrode) for 600 s upon deposition of 50 μL of a 1 mM $AuCl_4 \cdot 3H_2O$ solution prepared in 0.5 M H_2SO_4 [18]. The AuNPs/rGO/SPCEs were washed with Milli-Q H_2O and left to dry at room temperature. The electrodeposited AuNPs were modified with Fc-SH by exploiting the thiol chemistry through deposition of 10 μL of a 0.2 mg mL^{-1} Fc-SH solution (prepared in a mixture solution containing 1/5 ethanol and 0.1 M NaH_2PO_4/Na_2HPO_4 buffer solution, pH 7.0) during 8 h at room temperature in a humid chamber on the WE surface. After washing the electrode surface with methanol to remove the non-assembled Fc on the AuNPs and drying at room temperature, a 10 μL drop of a 0.2 mg mL^{-1} PCA solution was casted over the Fc-SH/AuNPs/rGO/SPCE WE and dried under an incandescent lamp.

Subsequently, the PCA/Fc-SH/AuNPs/rGO/SPCEs were covalently modified with NH_2-DNACp using carbodiimide/succinimide chemistry (EDC/NHS). Two successive 30 min-incubation steps at 4 °C in a humid chamber (separated by a washing with Milli-Q H_2O) were performed. The first incubation was made by placing onto the WE 10 μL drops of 2 mg mL^{-1} EDC and NHS solutions (freshly prepared in Tris-EDTA, pH 8.0). The second step involved dropping of a 10 μL aliquot of a 0.05 μM NH_2-DNACp solution (also in Tris-EDTA, pH 8.0) [19]. During this step, the NH_2-DNACp molecules are covalently attached to the PCA/Fc-SH/AuNPs/rGO/SPCE by forming an amide bond between their NH_2 terminated groups and the O-acylisourea intermediates generated upon activating PCA/rGO carboxylic groups with EDC/NHS [20]. After washing and drying the NH_2-DNACp/PCA/Fc-SH/AuNPs/rGO/SPCE, two successive blocking steps were performed by incubation with 10 μL of a 0.1 mM MCH solution (prepared in Tris-EDTA, pH 8.0) for 5 min and, thereafter, with 10 μL of a 1% (w/v) BSA solution (prepared also in Tris-EDTA, pH 8.0) for 1 h.

Target miRNA hybridization at the NH_2-DNACp/PCA/Fc-SH/AuNPs/rGO/SPCE

The target miRNA hybridization at the NH_2-DNACp/PCA/Fc-SH/AuNPs/rGO/SPCE was accomplished by casting a 10 μL aliquot of the target miRNA or the sample onto the WE and incubation at room temperature during 30 min.

Electrochemical measurements

The hybridization event with the target miRNA was monitored by recording DPVs between − 0.5 and + 0.6 V (vs. the Ag pseudo-reference electrode) at 10 mV s^{-1} upon placing a 50 μL drop of PBS (pH 7.0) on the SPCE covering the three electrodes area. All signals given in the manuscript correspond to the difference between the oxidation peak current of Fc-SH measured before and after performing the hybridization step (Δi).

The characterization of the stepwise biosensor preparation was made by EIS and CV. A 50 μL drop of a 5 mM $[Fe(CN)_6]^{3-/4-}$ solution supplemented with 0.1 M KCl was placed on the SPCE. EIS measurements were carried out at + 0.12 V (vs. Ag-pseudo-reference electrode), in a frequency range of 1 kHz to 0.01 Hz with a 0.01 V rms signal. CV experiments were performed at 50 mV s^{-1} over the − 0.4 to + 0.8 V potential range.

Error bars given through the manuscript were estimated as triple of the standard deviation of three replicates.

Direct determination of miRNA–21 in serum from breast cancer (BC) patients and in total RNA (RNA_t) extracted from BC cells

The biosensors were applied to the determination of the endogenous content of the target miRNA in serum samples from healthy individuals and patients diagnosed with BC provided by the Biology Department of the University of Tunis El Manar (Prof. Besma Loueslati) after obtaining the informed consent of the patients and the ethics committee approval of the institution. The protocol described in Target miRNA hybridization at the NH_2-DNACp/PCA/Fc-SH/AuNPs/rGO/SPCE was applied to 2 times diluted serum samples in sterilized PBS, pH 7.5, and heated for 15 min at 95 °C in a block heater to release the entrapped *miRNAs* from membrane vesicles [21]. After verifying the absence of matrix effect, the determination was made by simple interpolation of the obtained Δi-value into the calibration graph constructed with synthetic miRNA-21 standards.

The determination of miRNA-21 in RNA_t extracted from breast cells (both tumorigenic, MCF-7, and non-tumorigenic, MCF-10A) was accomplished by using the protocols previously described in [22, 23].

Results and discussion

Design of the biosensor

Scheme 1 shows a cartoon of the developed biosensor for the determination of miRNA-21. The bioplatform uses disposable carbon electrodes doubly nanostructured with rGO and AuNPs to take advantage of the excellent properties offered by these two nanomaterials in electrochemical biosensing. The rGO offers outstanding conducting properties, large surface area, biocompatibility, and functional ligands for further modification [24–26], and the AuNPs impart also the nanostructured surface improved conductivity, catalytic activity, and biocompatibility [27, 28]. In the particular approach presented, AuNPs were used for anchoring of the redox probe 6-ferrocenylhexanethiol (Fc-SH), and rGO was modified with PCA to enrich non-invasively rGO with carboxylic acid functionalities [25]. Since the carboxylic acid group in PCA is a moderate electron withdrawing group and the pyrene aromatic core is a good electron donor, the π-π stacking interactions of the pyrene core with the islands of graphene network favored the charge transfer from the PCA to the graphene. This electrode scaffold acted as building block for the covalent binding through EDC/NHS coupling reaction of a NH_2 terminated synthetic DNA capture probe (NH_2-DNACp) complementary to the target miRNA (the oncogenic miRNA-21). Upon blocking of the electrode surface to avoid possible non-specific adsorptions on the surface of unmodified Fc-SH AuNPs or activated PCA/rGO groups free of immobilized NH_2-DNACp, the target miRNA was probed by the decrease in the DPV oxidation signal of the Fc molecules attached to the surface after the hybridization step due to the partial blocking of the electrode surface.

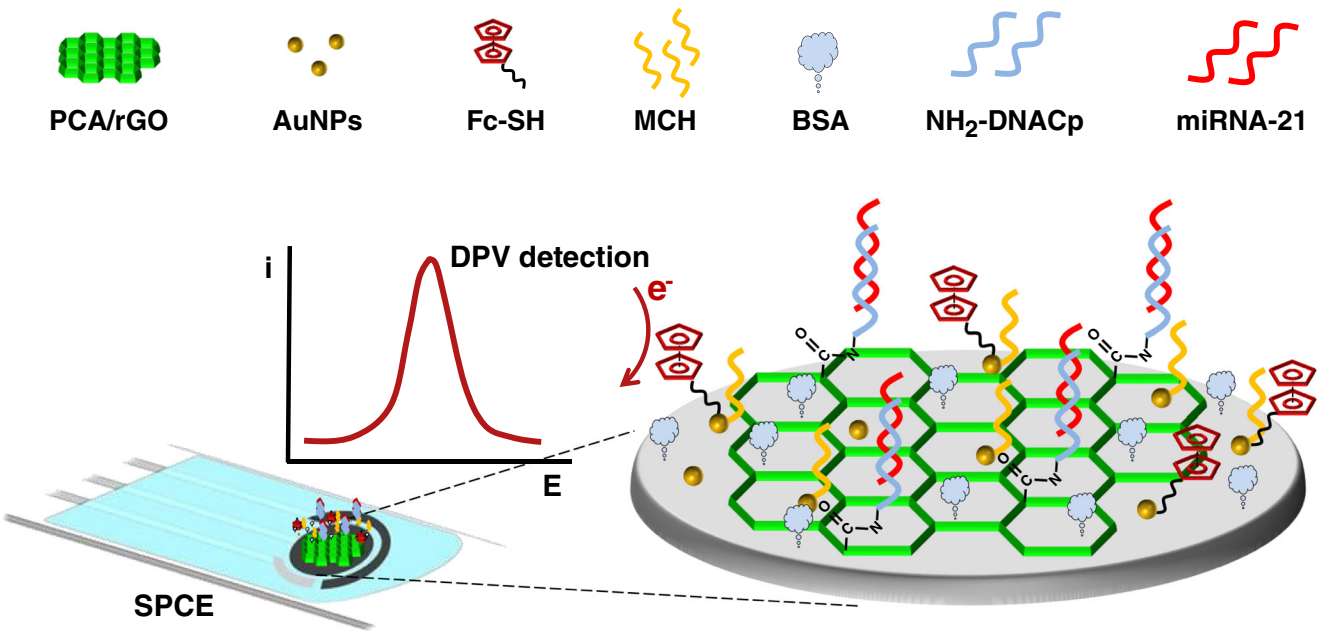

Scheme 1 Schematic diagram of the developed biosensor for the label-free voltammetric determination of miRNA-21 through the covalent immobilization of NH_2-DNACp on disposable electrodes nanostructured with rGO modified with PCA and AuNPs modified with Fc-SH, and the DPV detection of the Fc oxidation signal

Characterization of the modified SPCEs surfaces

The rGO/SPCE, AuNPs/rGO/SPCE, and Fc-SH/AuNPs/rGO/SPCE surfaces were characterized by SEM in our previous work confirming the double nanostructuring of SPCE with rGO and AuNPs [15]. Figure S1 (in the Supporting Material) displays the SEM and EDX analysis of Fc-SH/AuNPs/rGO/SPCE. The EDX results confirmed the presence of C, O, Fe, and Au, thus demonstrating the successful modification of the electrode substrates.

The reliability of the bioplatform and the role played by each component were checked by recording the DPV responses in the absence and in the presence of the target miRNA. DP voltammograms were obtained at NH_2-DNACp/PCA/Fc-SH/AuNPs/rGO/SPCE, PCA/Fc-SH/AuNPs/rGO/SPCE (control without DNA capture probe), and NH_2-DNACp/Fc-SH/AuNPs/rGO/SPCE (control without PCA). Figure 1 shows a large DPV response for the Fc oxidation provided by the NH_2-DNACp/PCA/Fc-SH/AuNPs/rGO/SPCE (black line in Fig. 1a), attributed to the large number of Fc molecules attached to the AuNPs and their close proximity to the underlying electrode [29–31]. In addition, Fig. 1 shows that it was not possible to discriminate the presence of the target miRNA at the PCA/Fc-SH/AuNPs/rGO/SPCEs (Fig. 1a) and the NH_2-DNACp/Fc-SH/AuNPs/rGO/SPCEs (Fig. 1b). These results confirmed that the decrease in the Fc oxidation DPV responses is due solely to the selective hybridization of miRNA-21with the covalently immobilized NH_2-DNACp onto PCA/rGO.

The stepwise electrode modification process was monitored by EIS and CV (Fig. 2a and b, respectively). As it can be seen in Fig. 2a, the charge transfer resistance (R_{ct}) of the SPCEs (3340 Ω) decreased upon modification with rGO (3225 Ω), AuNPs (2861 Ω), and Fc-SH (1061 Ω). These results are consistent with the enhanced electron transfer kinetics provided by the synergistic contribution of both nanomaterials [18] and the electrocatalytic properties [32] and/or positive charge of Fc-AuNPs [33]. All the following steps involving successive modifications with PCA (1481 Ω), BSA (2177 Ω), immobilization of NH_2-DNACp (2391 Ω), and hybridization with the target miRNA (2437 Ω) implied, as expected, slight increases in the R_{ct} values due to the insulating properties and/or the electrostatic repulsion between the negatively charged redox probe and the modified electrode surfaces. All these EIS results, also validated by the corresponding CV measurements (Fig. 2b), demonstrated the successful fabrication of the miRNA biosensor and are consistent with the role played by each component.

Optimization of the experimental variables

Key experimental variables such as the concentration of the capture probe, the time required for its covalent immobilization and the incubation time with the target miRNA to ensure its efficient hybridization at the bioplatform were evaluated. All these variables were optimized by comparing the difference between the oxidation peak current of Fc measured before and after hybridization with 2 pM miRNA-21 (Δi). The results displayed in Fig. S2 (in the Supporting Material) led us to select, as a compromise between sensitivity and assay time, a NH_2-DNACp concentration of 100 nM (Fig. S2a) and immobilization (Fig. S2b) and hybridization times (Fig. S2c) of 30 min.

Analytical performance

The DPV oxidation peak current of Fc noticeably decreased when increasing the miRNA-21 concentrations (Fig. 3) because the formation of the hybrids on the electrode surface hindered the electron transfer, thus allowing the label-free direct detection of the target miRNA. Figure 3 inset shows as the Δi value linearly increased with the miRNA-21 concentration from 18 fM to 2.0 pM (slope = 6.18 ± 0.07 μA pM^{-1}; intercept = 0.6 ± 0.6 μA; R^2 = 0.992). The

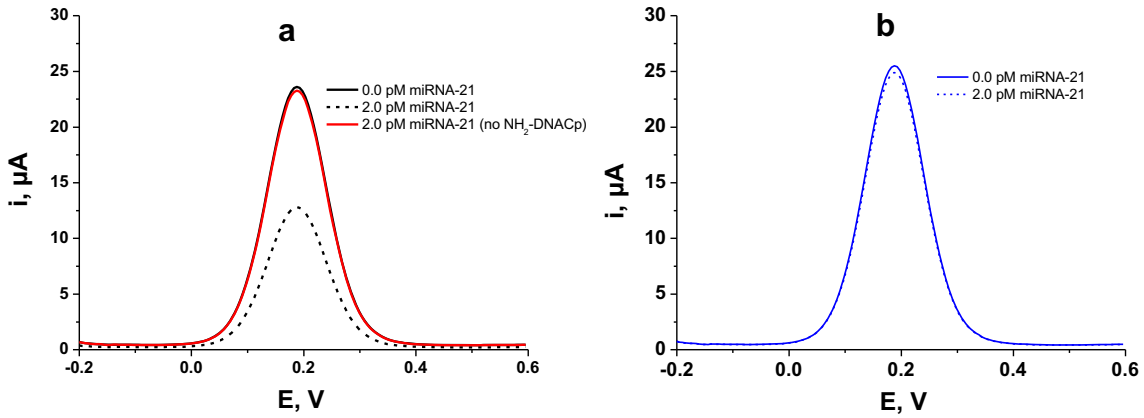

Fig. 1 DPV responses recorded in the absence and in the presence of 2.0 pM miRNA-21 at the NH_2-DNACp/PCA/Fc-SH/AuNPs/rGO/SPCE (black lines), the PCA/Fc-SH/AuNPs/rGO/SPCE (control without DNA capture probe, red line) (**a**), and the NH_2-DNACp/Fc-SH/AuNPs/rGO/SPCE (control without PCA, blue lines) (**b**)

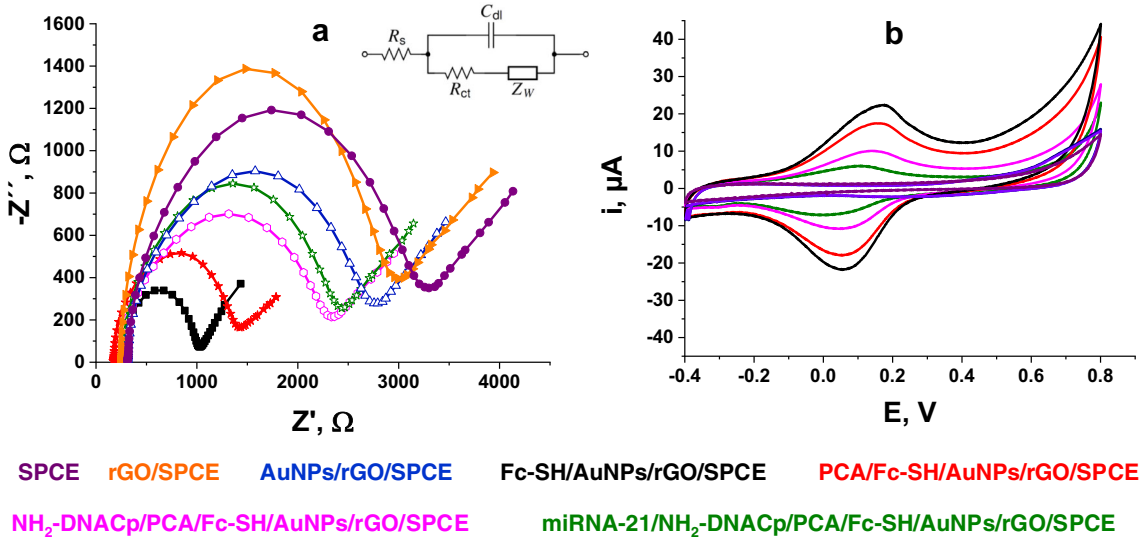

Fig. 2 Characterization of the stepwise biosensor fabrication by EIS (**a**) and CV (**b**). Nyquist plots and Randles' equivalent circuit (inset) (**a**) and CVs ($v = 50$ mV s^{-1}) (**b**) recorded at the modified electrodes using a 5 mM $[Fe(CN)_6]^{3-/4-}$ in 0.1 M KCl solution

LOD value, estimated according to the $3 \times s_b/m$ criterion, with s_b as the standard deviation of the DPV signals obtained in the absence of the target miRNA and m the slope of the calibration plot was 5.4 fM (equivalent to 54 zmol in 10 μL of sample). The high sensitivity achieved may be attributed to the large amount of $-CO_2H$ groups onto PCA/rGO, which allows large loadings of the NH_2-DNACp for miR-21, as well as to the use of AuNPs, which, apart from allowing convenient immobilization of Fc-SH through Au-S bond, provided the modified SPCE with improved conductivity (Fig. 2).

The analytical performance of the developed biosensor was compared with those claimed for other enzymeless electrochemical biosensors reported in the last 5 years for the label-free determination of miRNA-21 (Table 2). It can be concluded that the developed biosensor is attractive because of the achieved sensitivity using a simple (only 1 step) and short test time (30 min) protocol. In this context, it is important to note that although other methods claim lower LODs [11–14], some of them require more than 1 step [13] or multiple oligonucleotide probes and specific nucleases [14]. In addition, only one biosensor was constructed with disposable electrodes [13]. Moreover, all these more sensitive strategies demonstrated applicability for the determination in cellular RNA_t, and spiked or heavily diluted serum/blood samples, most of them requiring extended time to prepare the bioplatform. Furthermore, in comparison with another method recently developed to determine the endogenous content of miRNA-21 directly in serum [15], the method reported in this work provides a similar LOD but involves a simpler (1 vs. 3 steps) and shorter (30 min vs. 1 h 45 min) protocol to perform the determination. Importantly, the method proposed in this work involves a fully integrated bioplatform prepared in less time (9 vs. 24 h), and it does not require nanocarriers of signaling elements, whose preparation lasted than 24 h. All these features make this new biosensor more compatible with potential future implementation in point-of-care devices.

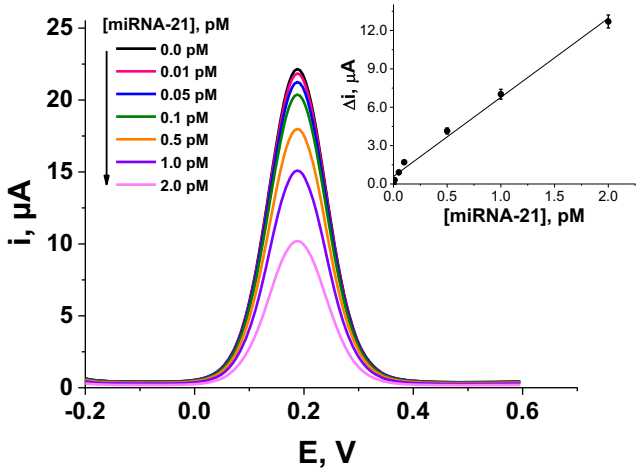

Fig. 3 DPV responses provided by the biosensor developed for the determination of miRNA-21 for different synthetic target concentrations and the resulting calibration plot (inset)

The responses obtained with 5 different biosensors prepared in the same way for a 2 pM miRNA-21 solution provided a RSD value of 4.5% (real data shown in Fig. S3 in the Supporting Material), indicating a noticeable reproducibility for all the involved protocols (manufacture of the biosensors, hybridization of the target miRNA on their surface, and electrochemical detection of the hybridization process).

Moreover, a study of the NH_2-DNACp/PCA/Fc-SH/AuNPs/rGO/SPCEs storage stability in dry conditions and at 4 °C was carried out. The responses provided by the biosensors each day of control in the absence and in the presence of 2 pM miRNA-21 showed that they remained within the control limits (set at $\pm 3 \times$ SD of the mean Δi values measured with five different sensors prepared on the first day of the

Table 2 Electrochemical biosensors reported in the last 5 years for the label-free determination of miRNA-21

Electrode	Fundamentals	Technique	Linear range/LOD	Time and number of steps required for miRNA determination/ biosensor fabrication time	Selectivity*	Storage stability**	Sample (amount)	Ref.
GCE modified with MWCNT-COOH	Direct adsorption of the DNACp on the MWCNT-COOH-GCE and direct hybridization with the target miRNA	DPV (MB)	0.1–500.0 pM/84.3 fM	1 h and 5 min (2 steps)/≥ 5 h	NC: ~ 20%	—	—	[34]
GCE modified with MoS_2-Thi-AuNPs	Immobilization of a SH-DNACp on a MoS_2-Thi-AuNPs-modified GCE and direct hybridization	SWV (Thi)	1.0 pM–10.0 nM/0.26 pM	50 min (1 step)/≥ 17 h	1-m: 39–53% NC: 5%	—	Spiked 1% human serum samples	[9]
AuE modified with AgNF and PPy	Immobilization of pyrrolidinyl peptide nucleic acid (acpcPNA) probe onto the PPy/AgNF/Au electrode and direct hybridization	CV (AgNF)	0.20 fM–1.0 nM/0.20 fM	15 min (1 step)/≥ 14 h	1-m: 7.5–11.7-% NC: 1.1–9.6-%	—	100-times diluted human serum samples	[11]
FTO electrode modified with a NFG/AgNPs/PANI nanocomposite	Covalent immobilization of an NH_2-DNACp at the NFG/AgNPs/PANI-modified FTO electrode and direct hybridization with the target miRNA	DPV	10 fM–10 μM/0.2 fM	30 min (1 step)/≥5 h 40 min	—	—	Spiked blood serum samples	[12]
Au-SPE	Adsorption of the target miRNA (previously isolated onto b-DNACp-Strep-MBs) on the Au-SPE	DPV ($[Fe(CN)_6]^{3-/4-}$)	1.0 pM–10 nM/1 pM	~ 1 h (4 steps)/—	—	—	50 ng RNA_t extracted from cancer cell exosomes	[35]
GO/IO NPs/SPCE	Adsorption of the target miRNA /b-DNACp heterohybrid (previously isolated onto Strep-MBs) on the GO/IO NPs/SPCE	Chronocoulometry ($[Ru(NH_3)_6]^{3+}$/ $[Fe(CN)_6]^{3-/4-}$)	1.0 fM–1.0 nM/1.0 fM	~ 2 h (4 steps)/—	NC: 0%	—	Ovarian cancer cells extracted RNA_t	[13]
AuE	Direct hybridization at a Cp-TSP-modified AuE and specific cleaved of DNA-RNA heterohybrids by DSN. The TSPs designed recognized both the target	DPV (TMB/H_2O_2)	0.1 fM–0.1 pM/0.04 fM	1 h (1 step)/~ 12 h 30 min	1-m: ~ 20%	2 weeks (94.2% of the original response)	Spiked 1% human serum samples	[14]

Table 2 (continued)

Electrode	Fundamentals	Technique	Linear range/LOD	Time and number of steps required for miRNA determination/ biosensor fabrication time	Selectivity*	Storage stability**	Sample (amount)	Ref.
	miRNA and a G-quadruplex sequence with biocatalytic functions for H_2O_2 reduction combined with hemin							
AuE	Direct hybridization at DNACp immobilized onto cross-shaped DNA origami nano structures (AuE/chitosan/ origami-DNACp)	DPV (MB)	0.1 M–10.0 nM/79.8 fM	~ 2 h 5 min (2 steps)/~ 16 h	1-m: ~ 84%, 2-m: ~ 57%	–	Spiked 1 % human serum samples	[6]
AuNPs/rGO/SPCE	Sandwich hybridization approach involving specific SH-DNACp and b-DNADp and Fc-AuNPs-Strep as nanocarriers of signaling elements	DPV (Fc)	10 fM–2 pM/5.0 fM	~ 1 h 45 min (3 steps)/~ 9 h 35 min + Fc-AuNPs-Strep (~ 24 h)	1-m: ~ 4%	≥ 2 months	50 ngRNA_t extracted from BC cells and 2 times diluted serum samples from BC patients	[15]
PCA/Fc-SH/ AuNPs/rGO/SPCE	Direct hybridization approach at NH_2-DNACp/PCA/Fc-SH/ AuNPs/rGO/SPCE	DPV (Fc)	18 fM–2.0 pM/5.4 fM	30 min (1 step)/~ 9 h	1-m: ~ 19%	≥ 2 months	2 times diluted serum samples from BC patients	This work

*,** % referred to the response provided for the target miRNA and by the biosensor on the day of its manufacture, respectively

AuE gold electrode; *AuNPs* gold nanoparticles; *b* biotin; *BC* breast cancer; *Cp* capture probe; *Dp* detector probe; *DPV* differential pulse voltammetry; *DSN* duplex-specific nuclease; *EIS* electrochemical impedance spectroscopy; *Fc* ferrocene; *Fc-AuNPs-Strep* AuNPs/Strep conjugates capped with 6-(ferrocenyl)hexanethiol; *GO/IO NPs* graphene oxide–loaded superparamagnetic iron oxide nanoparticles; *LOD* limit of detection; *1-m* single-base mismatched sequence; *MB* methylene blue; *MBs* magnetic microbeads; *NC* non-complementary sequence; *rGO* reduced graphene oxide; *RNA_t* total RNA; *SPCE* screen-printed carbon electrode; *Strep* streptavidin; *TMB* 3,3′,5,5′-tetramethylbenzidine; *TSP* tetrahedral DNA nanostructure probe

study) for at least 60 days (Fig. 4). This high storage stability can be attributed to both the stability of the covalent bonding [20] and the biocompatible interface nanostructured with AuNPs [36].

Selectivity

The selectivity of the biosensor was tested by comparing the responses in the presence of 2 pM miRNA-21 with those recorded for a full non-complementary (NC) sequence (the tumor suppressor miRNA-451), a single unpaired base (1-m) sequence, and a mixed solution containing both the target and the NC sequence at the same concentration. The corresponding DP voltammograms are displayed in Fig. 5, showing that the developed biosensor provided 1, 19, and 96% of the response obtained for the target miRNA, for the NC, 1-m, and miRNA-21/NC mixture, respectively, thus confirming a total discrimination against NC sequences and very favorable against 1-m sequences.

Determination of the miRNA–21 endogenous content in sera collected from BC patients

The biosensor was employed to quantify the endogenous content of miRNA-21 in serum samples from patients diagnosed with BC with no need for prior extraction of RNA_t. The possibility of performing the determination directly in undiluted serum was evaluated by comparing the slope values of the calibration graphs constructed with miRNA-21 buffered solutions and in undiluted or 2 to 5 times diluted serum samples from a healthy individual and a BC patient. No significant differences were apparent between the slope values calculated for calibration plots

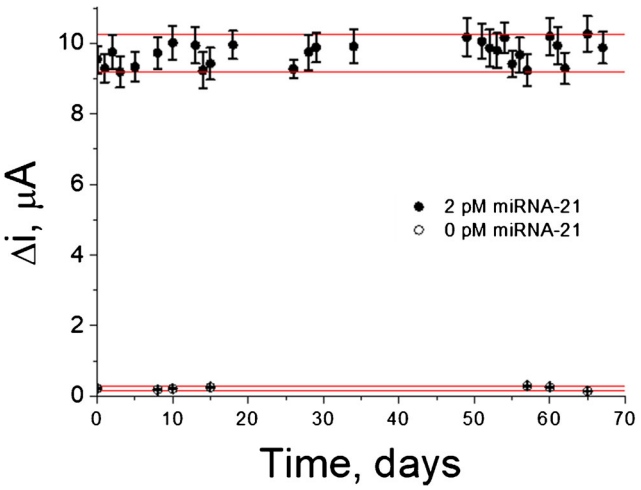

Fig. 4 Storage stability of the NH_2-DNACp/PCA/Fc-SH/AuNPs/rGO/SPCEs. Fc oxidation peak current values measured by DPV with the stored biosensors in the absence (empty circles) and in the presence (solid circles) of 2 pM miRNA-21 each control day counted since its preparation

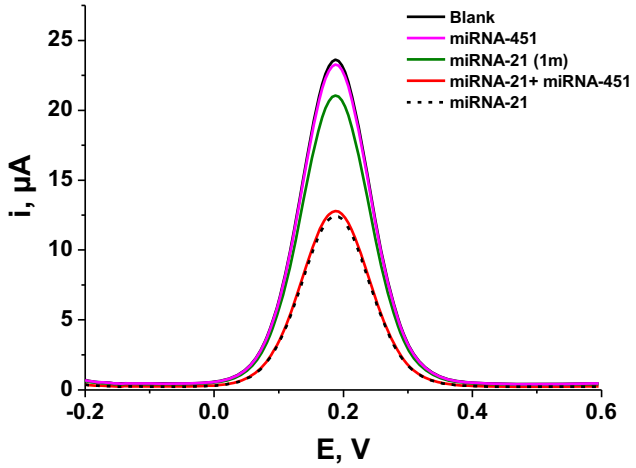

Fig. 5 Comparison of the DPV responses provided by the developed biosensor in the absence and in the presence of 2 pM miRNA-21, NC, and 1-m synthetic sequences and for the miRNA-21/NC mixture

in standard solutions (6.18 ± 0.07 μA pM^{-1}) and in 2 or more times diluted serum samples (6.49 ± 0.02 and 6.64 ± 0.05 μA pM^{-1} for a healthy individual and a BC patient, respectively, with t_{exp} values of 3.432 and 3.802, both lower than the t_{tab} value of 4.303, $n = 3$). These results indicated the absence of matrix effect in such diluted samples and allowed performing the quantification by simple interpolation of the responses obtained for the diluted samples into the calibration plot obtained with miRNA-21 standards. Using 2 times diluted samples, an endogenous content of miRNA-21 of 51 ± 6 fM was obtained for healthy individuals, while 126 ± 11 and 113 ± 9 fM were found in the sera of the two BC patients analyzed (see representative DPV traces in Fig. 6a). These results are in agreement with those obtained by other authors [11, 15] and show an overexpression of this oncomiRNA ~3 times higher in serum from patients diagnosed with BC compared with that found in healthy individuals [14, 37].

The biosensor was also used for the analysis of the endogenous content of miRNA-21 in RNA_t extracted from breast cells (Fig. 6b). Quantification was possible using only 50 ng of RNA_t and without matrix effect (slope value of 6.59 ± 0.03 μA pM^{-1} for the calibration plot prepared in the presence of 50 ng RNA_t extracted from MCF-10A, $t_{exp} = 3.721 < t_{tab} = 4.303$). The endogenous contents of miRNA-21 calculated by interpolating the amperometric responses provided by the biosensors for 50 ng of cellular RNA_t into the calibration graph constructed with miRNA-21 standard solutions were 0.9 ± 0.1 and 3.7 ± 0.3 amol ng^{-1} in MCF-10A and MCF-7, respectively. Again, these results are in good agreement with those reported using other electrochemical biosensors [37, 38] as well as using completely different methodologies [39, 40], thus confirming the accuracy of the biosensor developed.

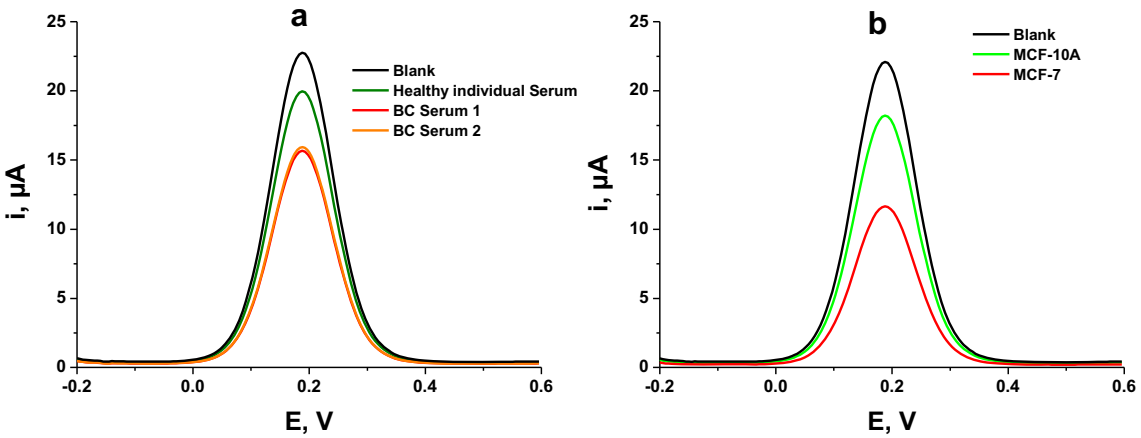

Fig. 6 Representative DPV traces recorded with the developed biosensor in the absence of miRNA-21 (blank signal) and in the presence of 2 times diluted serum samples from a healthy individual and two BC patients (**a**) or for 50 ng of RNA_t extracted from breast cells (**b**)

Conclusions

This work reports a new biosensor involving a one-step preparation and label-free approach for the sensitive and selective voltammetric determination of miRNAs in only 30 min. The biosensing platform is implemented on SPCE nanostructured with rGO and AuNPs serving as scaffolds for the immobilization of a NH_2-DNACp complementary to the target miRNA (miRNA-21) after modification with PCA and activation with EDC/NHS and Fc-SH, respectively. These electrode modifiers empower the biosensor with a high sensitivity and effectiveness to distinguish single-base mismatched sequences by adopting the decrease in the Fc DPV oxidation signal upon efficient hybridization at the electrode surface as the analytical readout. The proposed electrochemical biosensor is competitive in terms of simplicity and affordability against other label-free developed biosensors which involve complex multistep fabrication and/or multiple probes and specific enzymes. Interestingly, the biosensor allows determining the target miRNA in a small amount of RNA_t extracted from BC cells (50 ng) or 2 times diluted BC serum samples, without prior extraction, purification, amplification, or reverse transcription of the RNA material. The reported method combines a good analytical performance (sensitivity, specificity, and versatility to determine any microRNA) with the manufacturing and detection possibilities offered by mass fabricated SPEs and current electrochemical instruments and a high usability (high throughput, simplified workflow, and cost-effectiveness). These unique features make the developed biosensor to approach closely the required needs to implement miRNAs determination into clinical workflows for cancer diagnosis and assessment at the point of attention for the benefit of patients.

Funding information The Tunisian Ministry of Higher Education and Scientific Research (Lab. LR99ES15). NR thanks the Tunisian PRF program for financial support (**NanoFastResponse** ref. PRF2017-D4P1, **SmartBioSens** ref. PRFCOV19-D2P2 and **COVID-PP** ref. PRFCOV19-D3P1) and Prof. Besma Loueslati (University of Tunis El Manar, Biology department) for providing the serum samples used in this study. Ministerio de Ciencia e Innovación Project, PID2019-103899RB-I00 and the TRANSNANOAVANSENS−CM Program from the Comunidad de Madrid (Grant S2018/NMT−4349) are gratefully acknowledged.

Compliance with ethical standards

Conflict of interests The authors declare no conflict of interest. The funders had no role in the design of the study; in the collection, analyses, or interpretation of data; in the writing of the manuscript; or in the decision to publish the results.

References

1. Ling H, Fabbri M, Calin GA (2013) MicroRNAs and other non-coding RNAs as targets for anticancer drug development. Nat Rev Drug Discov 12(11):847–865. https://doi.org/10.1038/nrd4140
2. Tufman A, Tian F, Huber RM (2013) Can MicroRNAs improve the management of lung cancer patients? A Clinician's perspective. Theranostics 3(12):953–963
3. Berger F, Reiser MF (2013) Micro-RNAs as potential new molecular biomarkers in oncology: have they reached relevance for the clinical imaging sciences? Theranostics 3(12):943–952
4. Kappel A, Keller A (2017) miRNA assays in the clinical laboratory: workflow, detection technologies and automation aspects. Clin Chem Lab Med 55(5):636–647
5. Bellassai N, D'agata R, Jungbluth V, Spoto G (2019) Surface plasmon resonance for biomarker detection: advances in non-invasive cancer diagnosis. Front Chem 7:570
6. Han S, Liu W, Yang S, Wang R (2019) Facile and label-free electrochemical biosensors for MicroRNA detection based on DNA origami nanostructures. ACS Omega 4(6):11025–11031
7. Islam MN, Masud MK, Nguyen N-T, Gopalan V, Alamri HR, Alothman ZA, Al Hossain MS, Yamauchi Y, Lamd AK, Shiddiky MJ (2018) Gold-loaded nanoporous ferric oxide nanocubes for electrocatalytic detection of microRNA at attomolar level. Biosens Bioelectron 101:275–281
8. Li J, Fu W, Wang Z, Dai Z (2019) Substrate specificity-enabled terminal protection for direct quantification of circulating MicroRNA in patient serums. Chem Sci 10(21):5616–5623
9. Zhu D, Liu W, Zhao D, Hao Q, Li J, Huang J, Shi J, Chao J, Su S, Wang L (2017) Label-free electrochemical sensing platform for

microRNA-21 detection using thionine and gold nanoparticles co-functionalized MoS2 nanosheet. ACS Appl Mater Interfaces 9(41): 35597–35603
10. Cui F, Zhou Z, Zhou HS (2019) Measurement and analysis of cancer biomarkers based on electrochemical biosensors. J Electrochem Soc 167(3):037525
11. Kangkamano T, Numnuam A, Limbut W, Kanatharana P, Vilaivan T, Thavarungkul P (2018) Pyrrolidinyl PNA polypyrrole/silver nanofoam electrode as a novel label-free electrochemical miRNA-21 biosensor. Biosens Bioelectron 102:217–225
12. Salahandish R, Ghaffarinejad A, Omidinia E, Zargartalebi H, Majidzadeh-A K, Naghib SM, Sanati-Nezhad A (2018) Label-free ultrasensitive detection of breast cancer miRNA-21 biomarker employing electrochemical nano-genosensor based on sandwiched AgNPs in PANI and N-doped graphene. Biosens Bioelectron 120: 129–136
13. Islam MN, Gorgannezhad L, Masud MK, Tanaka S, Hossain MSA, Yamauchi Y, Nguyen NT, Shiddiky MJ (2018) Graphene-oxide-loaded superparamagnetic iron oxide nanoparticles for ultrasensitive electrocatalytic detection of MicroRNA. ChemElectroChem 5(17):2488–2495
14. Lu J, Wang J, Hu X, Gyimah E, Yakubu S, Wang K, Wu X, Zhang Z (2019) Electrochemical biosensor based on tetrahedral DNA nanostructures and G-quadruplex–hemin conformation for the ultrasensitive detection of MicroRNA-21 in serum. Anal Chem 91(11):7353–7359
15. Zouari M, Campuzano S, Pingarrón JM, Raouafi N (2020) Femtomolar direct voltammetric determination of circulating miRNAs in sera of cancer patients using an enzymeless biosensor. Anal Chim Acta 1104:188–198
16. Martin C, Grgicak C (2014) The effect of repeated activation on screen-printed carbon electrode cards. ECS Trans 61(26):1–8
17. Chen L, Tang Y, Wang K, Liu C, Luo S (2011) Direct electrodeposition of reduced graphene oxide on glassy carbon electrode and its electrochemical application. Electrochem Commun 13(2):133–137
18. Hu Y, Jin J, Wu P, Zhang H, Cai C (2010) Graphene–gold nanostructure composites fabricated by electrodeposition and their electrocatalytic activity toward the oxygen reduction and glucose oxidation. Electrochim Acta 56(1):491–500
19. Mercier D, Haddada MB, Huebner M, Knopp D, Niessner R, Salmain M, Proust A, Boujday S (2015) Polyoxometalate nanostructured gold surfaces for sensitive biosensing of benzo [a] pyrene. Sensors Actuators B Chem 209:770–774
20. Rashid JIA, Yusof NA (2017) The strategies of DNA immobilization and hybridization detection mechanism in the construction of electrochemical DNA sensor: a review. Sens Biosensing Res 16:19–31
21. Labib M, Khan N, Ghobadloo SM, Cheng J, Pezacki JP, Berezovski MV (2013) Three-mode electrochemical sensing of ultralow microRNA levels. J Am Chem Soc 135(8):3027–3038
22. Campuzano S, Torrente-Rodríguez RM, López-Hernández E, Conzuelo F, Granados R, Sánchez-Puelles JM, Pingarrón JM (2014) Magnetobiosensors based on viral protein p19 for microRNA determination in cancer cells and tissues. Angew Chem Int Ed 53(24):6168–6171
23. Torrente-Rodríguez R, Campuzano S, López-Hernández E, Granados R, Sánchez-Puelles J, Pingarrón J (2014) Direct determination of miR-21 in total RNA extracted from breast cancer samples using magnetosensing platforms and the p19 viral protein as detector bioreceptor. Electroanalysis 26(10):2080–2087
24. Singh R, Hong S, Jang J (2017) Label-free detection of influenza viruses using a reduced graphene oxide-based electrochemical immunosensor integrated with a microfluidic platform. Sci Rep 7. https://doi.org/10.1038/srep42771
25. Zaharie-Butucel D, Potara M, Craciun A, Boukherroub R, Szunerits S, Astilean S (2017) Revealing the structure and functionality of graphene oxide and reduced graphene oxide/pyrene carboxylic acid interfaces by correlative spectral and imaging analysis. Phys Chem Chem Phys 19(24):16038–16046
26. Tarcan R, Todor-Boer O, Petrovai I, Leordean C, Astilean S, Botiz I (2020) Reduced graphene oxide today. J Mater Chem C 8(4):1198–1224. https://doi.org/10.1039/c9tc04916a
27. Campuzano S, Yanez-Sedeno P, Pingarron JM (2019) Nanoparticles for nucleic-acid-based biosensing: opportunities, challenges, and prospects. Anal Bioanal Chem 411(9):1791–1806. https://doi.org/10.1007/s00216-018-1273-6
28. Luo XL, Morrin A, Killard AJ, Smyth MR (2006) Application of nanoparticles in electrochemical sensors and biosensors. Electroanalysis 18(4):319–326. https://doi.org/10.1002/elan.200503415
29. Wang J, Li J, Baca AJ, Hu J, Zhou F, Yan W, Pang D-W (2003) Amplified voltammetric detection of DNA hybridization via oxidation of ferrocene caps on gold nanoparticle/streptavidin conjugates. Anal Chem 75(15):3941–3945
30. Baca AJ, Zhou F, Wang J, Hu J, Li J, Wang J, Chikneyan ZS (2004) Attachment of ferrocene-capped gold nanoparticle/streptavidin conjugates onto electrode surfaces covered with biotinylated biomolecules for enhanced voltammetric analysis. Electroanalysis 16(1–2):73–80
31. Lu H, Wu L, Wang J, Wang Z, Yi X, Wang J, Wang N (2018) Voltammetric determination of the Alzheimer's disease-related ApoE 4 gene from unamplified genomic DNA extracts by ferrocene-capped gold nanoparticles. Microchim Acta 185(12):549
32. Malvano F, Pilloton R, Albanese D (2018) Sensitive detection of Escherichia coli O157: H7 in food products by impedimetric immunosensors. Sensors 18(7):2168
33. Kwon D, Jeong H, Chung BH (2011) Label-free electrochemical detection of human α-thrombin in blood serum using ferrocene-coated gold nanoparticles. Biosens Bioelectron 28(1):454–458
34. Rafiee-Pour H-A, Behpour M, Keshavarz M (2016) A novel label-free electrochemical miRNA biosensor using methylene blue as redox indicator: application to breast cancer biomarker miRNA-21. Biosens Bioelectron 77:202–207
35. Boriachek K, Umer M, Islam MN, Gopalan V, Lam AK, Nguyen N-T, Shiddiky MJ (2018) An amplification-free electrochemical detection of exosomal miRNA-21 in serum samples. Analyst 143(7):1662–1669
36. Vidotti M, Carvalhal RF, Mendes RK, Ferreira D, Kubota LT (2011) Biosensors based on gold nanostructures. J Braz Chem Soc 22(1):3–20
37. Zouari M, Campuzano S, Pingarrón JM, Raouafi N (2018) Amperometric biosensing of miRNA-21 in serum and cancer cells at nanostructured platforms using anti-DNA–RNA hybrid antibodies. ACS Omega 3(8):8923–8931
38. Zouari M, Campuzano S, Pingarrón J, Raouafi N (2018) Ultrasensitive determination of microribonucleic acids in cancer cells with nanostructured-disposable electrodes using the viral protein p19 for recognition of ribonucleic acid/microribonucleic acid homoduplexes. Electrochim Acta 262:39–47
39. Xu F, Yang T, Chen Y (2016) Quantification of microRNA by DNA–peptide probe and liquid chromatography–tandem mass spectrometry-based quasi-targeted proteomics. Anal Chem 88(1):754–763
40. Liu M, Hui CY, Zhang Q, Gu J, Kannan B, Jahanshahi-Anbuhi S, Filipe CD, Brennan JD, Li Y (2016) Target-induced and equipment-free DNA amplification with a simple paper device. Angew Chem Int Ed 55(8):2709–2713